Available online at www.sciencedirect.com
SCIENCE DIRECT®
Journal of Hydrology 279 (2003) 70–82
Journal of Hydrology
www.elsevier.com/locate/jhydrol

Unsaturated quasi-linear flow analysis in V-shaped domains

A.R. Kacimov*

Department of Soil and Water Sciences, Sultan Qaboos University, P.O. Box 34, Al-Khod 123, Sultanate of Oman

Received 29 May 2002; accepted 23 April 2003

Abstract

An explicit, essentially 2D solution for steady unsaturated seepage flow from infinity to a corner, with boundaries kept at constant suction, is obtained for the Kirchhoff potential by the method of separation of variables. A system of coordinates coinciding with the corner boundaries is selected. Distributions of the pressure, stream lines and velocities are derived. Non-existence of steady flows at certain corner orientations, deflection of the incident flow by slanted boundaries and inflection points on the stream lines close to the vertex are discussed. One-dimensional limit for zones far from the trough is examined. Refraction and further collimation of the upper 2D flow in the second underlying porous medium with implications to geotechnical capillary barriers is studied. A vadose zone originated accretion is matched with a saturated 'wing', which appears on a slanted bedrock. Mathematically, this matching is done by linking the Dupuit–Forchheimer and quasi-linear models. A tilted water table is shown to entrain the recharging moisture with curvilinear stream lines in the unsaturated zone.

Keywords: Unsaturated flow; Capillary barrier; Seepage; Suction; Recharge; Water table

1. Introduction

Descending (infiltration) and ascending (evaporation and capillary rise) unsaturated flows in porous media control distributions of moisture content, matrix potential, solute concentration, mechanical stresses and other physical parameters, which are studied, for example, in hydrology, irrigation and drainage, environmental physics and geomechanics. Theoretical description of these flows is impeded by two obstacles. First, even in steady conditions and homogeneous media flow is described by highly non-linear partial differential equations (PDEs), the non-linearity of which originates from a compound interrelation between conductivity, pressure and degree of saturation (Philip, 1969). Second, soils or rocks are naturally composed of zones with contrasting textural and structural properties. This heterogeneity, even if detected appropriately in the field, can be analytically taken into account in a few simple flow schemes for which the PDEs are solvable.

The paucity of geological and pedological information on heterogeneity and intrinsic mathematical problems in solution of PDEs is obviated by conceptualizing the subsurface as a laminated system. Horizons in soil physics, commingled formations in petroleum geology or interbedded aquifers-aquitards in groundwater hydrology are postulated to have piece-wise constant parameters, which change abruptly across horizontal interfaces. However, the undulating division boundaries between two adjacent

* Tel.: +968-515-223; fax: +968-513-418.
E-mail address: anvar@squ.edu.om (A.R. Kacimov).

0022-1694/03/$ - see front matter © 2003 Elsevier B.V. All rights reserved.
doi:10.1016/S0022-1694(03)00172-0

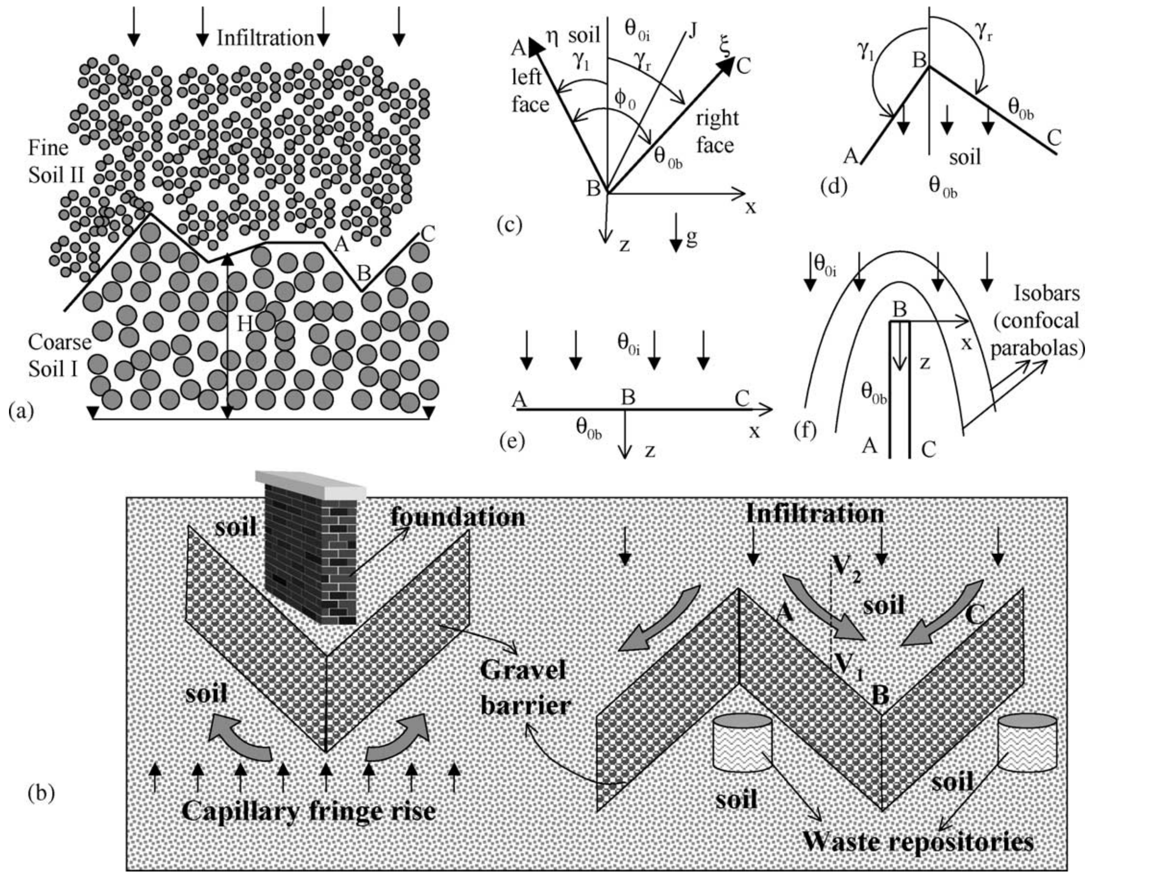

Fig. 1. (a) Infiltration through a two-layer soil, (b) exfiltration and infiltration near crenellated geotechnical barriers, (c) trough geometry, (d) protrusion, (e) flat draining layer, (f) constant pressure slot.

materials in natural soils or rocks as in Fig. 1 are more common than straight ones. Man-made engineering constructions (gravel packs, draining layers or clay liners) are often purposely shaped with edges, corrugations or zigzags as in Fig. 1b (Cedergren, 1989). For example, capillary barriers are used to protect landfills, waste repositories, basements, etc. against moisture fluxes (Ross, 1990; Khire et al., 2000). The main element of these barriers is a coarse wedge two flanks of which divert the incident flow from a protected area under the apexes. The re-routed water seeps into troughs where it does not inflict any damage (e.g. to a waste repository as in Fig. 1b). In agriculture, planting is also made in natural dimples or dug excavations filled with a porous medium, the properties of which contrast with the parent material. Thus, geologically born irregularities on natural interfaces or crenellated profiles in designed subsurface structures call for models more adequate than ideal strata.

The practical motivation of this paper is to study 2D unsaturated flows in depressions or protrusions as *ABC* in Fig. 1a and to answer the following question: what is the distribution of the matrix potential, stream lines and velocities in the trough zone depending on the incident infiltration intensity, physical properties of the two contrasting soils, the orientation of the trough and the obliquity of its two faces? In particular, we are interested in how much moisture can be accumulated (diverted) near (from) the trough vertex and how efficiently the trough pointedness thwarts gravity from bringing moisture into certain areas. Of special importance is the very existence of unsaturated flows and conditions when saturated wedges form on dome-type saliences of bedrock. In particular, we want to understand how the water table in a hillslope receives moisture from the unsaturated zone, when the groundwater zone is hidden under the slope surface and at which conditions a perched saturated zone exudes into the atmosphere.

The above mentioned mathematical non-linearity of the governing PDE for unsaturated flows has been effectively detoured by J.R. Philip and his colleagues via the so-called Gardner-soil model that posits an exponential dependence of the hydraulic conductivity on suction pressure. In that quasi-linear model, a non-linear PDE is reduced to the Helmholtz linear equation for which a machinery of known methods of wave mechanics (in particular optics) (Morse and Feshbach, 1953) has been applied (Philip, 1989a; Philip et al., 1989; Waechter and Philip, 1985), with a number of mathematically equivalent (and antedated) results available in the theory of heat transfer (e.g. Sretensky, 1935; Concer, 1959). For the 2D Helmholtz equation, explicit solutions have been obtained in domains where the equation separates, in particular, for an isobaric and impermeable cylinder (Philip, 1984) and parabola (Philip and Knight, 1989). For these geometries the PDE can be decoupled into two solvable ordinary differential equations (ODEs) that enables one to obtain explicit expressions for all flow characteristics. For more complicated shapes, Philip (1990a,b) cut 'the Gordian knot of separability' by applying the boundary layer approximation.

To the best of my knowledge, quasi-linear flows in corners as ABC (Fig. 1) have not been analyzed, although in these domains the Helmholtz equation either separates, i.e. reduces to two ODE, or can be treated by the normal mode expansion (Pinsky, 1991). This gap is strange because domains with corners and cusps are common in continuum mechanics. The behaviour of characteristic functions in these fundamental analytic elements (Strack, 1989) has been thoroughly studied in problems governed by the Laplace (saturated seepage, Polubarinova-Kochina, 1962), Poisson (flows in straight capillary tubes, Sisavath et al., 2001), biharmonic (viscous flows, Sherman, 1990), wave equations (diffraction of acoustical signals on sharp edges, Morse and Feshbach, 1953), etc.

A theoretical objective of our work is to obtain a new rigorous 2D solution, which in the limit can be reduced to 1D refraction on a sloped interface between soils of contrasting texture (Warrick et al., 1997). In particular, we can determine how far from point B in Fig. 1, the Ross (1990) deflection formula for a capillary barrier can be applied. We also discovered a simple example of an unconfined corner-shaped steady Dupuit–Forchheimer (DF) groundwater flow accruing moisture through a dipping water table, which, in its own turn, causes deformation of the infiltration streamlines.

2. Philip's model in non-orthogonal coordinates

We consider infiltration from above in a corner ABC with an angle of ordination ϕ_0 (Fig. 1c). We originate a Cartesian system of coordinates at the vertex B with z axis oriented downward. Soil fills the space between the left and right arms of the corner oriented at angles γ_l and $\gamma_r = \phi - \gamma_l$. The left angle is counted from $-z$ axis counterclockwise while the right angle—clockwise. We assume that along AB and BC pressure is a fixed constant, p_b. As will be discussed later, this corresponds to two-layered soils (Section 5). In a particular case when p_b is atmospheric, we match saturated and unsaturated flows by continuity of the normal and tangential flux components along the water table. If we move to infinity along any ray BJ originating at B and contained between AB and BC, then pressure tends to another constant, p_i. Both p_i and p_b are arbitrary but negative to ensure unsaturated conditions.

In the quasi-linear model, the hydraulic conductivity k is the Gardner (1958) function

$$k = k_s \exp(\alpha P)$$

where k_s is the saturated hydraulic conductivity, α is the sorptive number, $P = p/(\rho g)$ is the matrix potential expressed as a length, ρ is the fluid density, and g is the gravity acceleration. We assume that the soil is homogeneous and isotropic and hence α and k_s are constants. The Kirchhoff potential θ_0 is defined as

$$\theta_0 = \int_{-\infty}^{P} k(P)\mathrm{d}P = \frac{k_s \exp(\alpha P)}{\alpha}$$

From this expression we see that both pressure and potential are constant along ABC, i.e. $\theta_0 = \theta_{0b} = (k_s \exp \alpha P_b)/\alpha$. At infinity, excluding the domain boundaries AB and BC, the potential $\theta_0 = \theta_{0i} = (k_s \exp \alpha P_i)/\alpha$. In the quasi-linear model in general, θ_0 varies in the range $0 < \theta_0 < \theta_s$ where $\theta_s = k_s/\alpha$ corresponds to the complete saturation limit.

In our Cartesian coordinates, the reduced potential $\theta = \theta_0 - \theta_{0b}$ satisfies the following equation:

$$\frac{\partial^2\theta}{\partial x^2} + \frac{\partial^2\theta}{\partial z^2} - \alpha\frac{\partial\theta}{\partial z} = 0 \quad (1)$$

Although soils seldom exhibit perfectly Gardner conductivities, Philip invoked it as an expedient approximation leading to a linear PDE (1).

The homogeneous Dirichlet boundary condition and condition at infinity are

$$\theta_{ABC} = 0, \qquad \theta_i = \theta_{0i} - \theta_{0b} \quad (2)$$

We notice that if $\alpha = 0$ in Eq. (1), then Eqs. (1) and (2) has only a trivial solution when $\theta = \text{const}$ everywhere in the corner. Indeed, if a harmonic ($\alpha = 0$) function θ vanishes at the sides of an unbounded sector, then θ must grow to infinity at infinity. This is the crux of the famous Phragmen–Lindelof principle (Protter and Weinberg, 1984, pp. 93–96).

In order to find a non-trivial solution to the boundary value problem (1) and (2) at non-degenerating $\alpha > 0$, we combine the ideas and techniques from Philip (1998) and Warrick et al. (1997). As in Philip (1990b), we introduce a non-Cartesian (but 'natural') system of coordinates $\xi B \eta$:

$$\xi = \alpha(x\cos\gamma_l - z\sin\gamma_l),$$
$$\eta = -\alpha(x\cos\gamma_r + z\sin\gamma_r) \quad (3)$$

axes of which coincide with the corner sides. In these coordinates, Eq. (1) is transformed into the following PDE

$$\frac{\partial^2\theta}{\partial\xi^2} + \frac{\partial^2\theta}{\partial\eta^2} + 2B\frac{\partial^2\theta}{\partial\xi\,\partial\eta} + D\frac{\partial\theta}{\partial\xi} + E\frac{\partial\theta}{\partial\eta} = 0 \quad (4)$$

where $B = \cos(\pi - \phi_0)$, $D = \sin\gamma_l$ and $E = \sin\gamma_r$ are three constants.

Usually, PDEs of type (4) are reduced to Eq. (1) (Zauderer, 1989) or even to the so-called canonical form (the Helmholtz equation for an elliptic PDE) but, as we assert, for the corner problem a seemingly awkward Eq. (4) does provide some clues to solve Eqs. (1) and (2).

3. Right angle trough

We attempt to solve Eq. (4) by separation of variables searching for particular solutions in the form $\theta_m = F_m(\xi)G_m(\eta)$. Then we can easily separate our PDE if $\phi_0 = \pi/2,\ 3\pi/2$ when $B = 0$. Consequently, we arrive at two ODEs

$$F''_m + DF'_m - \lambda_m F_m = 0,$$
$$G''_m + EG'_m + \lambda_m G_m = 0 \quad (5)$$

where λ_m is the separation constant and $'$ designates differentiation with respect to the corresponding variable. The general solution to Eq. (5) is:

$$F_m = c_1\exp[-\xi/2(D + \sqrt{D^2 + 4\lambda_m})] + c_2\exp[\xi/2(-D + \sqrt{D^2 + 4\lambda_m})]$$
$$G_m = c_3\exp[-\eta/2(E + \sqrt{E^2 + 4\lambda_m})] + c_4\exp[\eta/2(-E + \sqrt{E^2 + 4\lambda_m})] \quad (6)$$

We assume now $\phi_0 = \pi/2$, $\gamma_r < \pi/2$ and $\gamma_l < \pi/2$ that corresponds to V-troughs as in Fig. 1c. Then it can be easily proved that the only opportunity for solutions (6) to satisfy the boundary and infinity conditions (2) is to set $\lambda_m = 0$. Therefore, $F_m = F = c_1\exp(-D\xi) + c_2$ and $G_m = G = c_3\exp(-E\eta) + c_4$. Using Eq. (2) we determine the constants c_{1-4} and arrive at

$$\theta = \theta_i[1 - \exp(-\xi\sin\gamma_l)][1 - \exp(-\eta\sin\gamma_r)] \quad (7)$$

Note that if $\gamma_r > \pi/2$ or $\gamma_l > \pi/2$ (situation shown in Fig. 1d), then from Eq. (6) we can deduce that the problem (1), (2) (or (2), (4)) has no non-trivial solutions (the trivial solution is 1D $\theta(x,z) = 0$ or in the original variables $\theta_0(x,z) = \theta_{0b} = \theta_{0i}$). This non-existence of descending non-uniform steady-state regimes is clear from Philip (1991) solution to the transient infiltration problem in a hill. Indeed, by supplying constant pressure on the hill sides in Fig. 1d we eventually saturate the whole soil volume up to the degree maintained at the surface and asymptotically (in time) reach a constant flux uniform descending infiltration.

Using Eq. (3) we can easily express θ through the original coordinates x and z. We stress that (7) remains inherently 2D in any coordinates, whereas some Philip's solutions (e.g. for a parabola) were 1D either in an appropriate system of coordinates or due to boundary-layer approximations.

Since γ_l, γ_r in Eq. (7) appear symmetrically, we shall focus (without any loss of generality) on the case $\gamma_l = \gamma_r = \pi/4$. Then from Eqs. (3) and (7)

$$\theta_0 = \theta_{0b} + (\theta_{0i} - \theta_{0b})[1 + \exp(\alpha z) - \exp(-\alpha/2(x - z)) - \exp(\alpha/2(x + z))] \quad (8)$$

The horizontal and vertical components of velocity can be found from Eq. (8)

$$u = -\frac{\partial \theta_0}{\partial x} = \alpha(\theta_{0i} - \theta_{0b})\exp(\alpha z/2)\sinh(\alpha x/2)$$
$$v = \alpha\theta_0 - \frac{\partial \theta_0}{\partial z} = \alpha\theta_{0i} + \alpha(\theta_{0i} - \theta_{0b})\exp(\alpha z/2)\cosh(\alpha x/2) \quad (9)$$

From Eq. (9) we can reconstruct lines of constant velocity magnitude. For instance, at $\theta_{0i} = 0$ these lines can be determined explicitly from $V = \sqrt{u^2 + v^2} = \alpha\theta_{0b}\exp(\alpha z/2)\sqrt{\cosh(\alpha x)} = \text{const}$. They are important to estimate stability of soil particles at textural interfaces, which are subjected to hydraulic gradients. Sufusion and clogging triggered by water carrying fine soil particles to a coarse material are limiting factors in the design of gravel packs (Cedergren, 1989). In our case it might become a problem (Philip, 1998) at $\theta_{0i} < \theta_{0b}$ when both seepage and gravity jointly act against cohesion (particle clinging) induced by capillary pendulae bridging two neighbouring grains.

A stream function $\psi(x, y)$ can be defined as $u = -\psi_z$, $v = \psi_x$. Integration of Eq. (9) yields:

$$\psi = \alpha\theta_{0i}x - 2(\theta_{0i} - \theta_{0b})\exp(\alpha z/2)\sinh(\alpha x/2) \quad (10)$$

with $\psi = 0$ assumed along $x = 0$.

Fig. 2a shows contour plots $\theta_0(x, z)$ and $\psi(x, z)$ for our symmetrically oriented trough at $\theta_{0i} = 0.1$, $\theta_{0b} = 1$ and $\alpha = 1$ (equivalent to introduction of dimensionless coordinates αx, αz and $\alpha\theta/k_s$). The equipotentials are depicted starting from 1 with a decrement of 0.1, and stream lines ranging from -2 to 2 with an increment of 0.2. Fig. 2b represents the same plots but for $\theta_{0i} = 1$ and $\theta_{0b} = 0.3$ As we can infer from Fig. 2 at $\theta_{0i} < \theta_{ob}$ and $|x| > x_c$, streamlines have an inflection point above the trough bottom. A precise location of inflection points can be found from the solution of a simple non-linear equation. We note that the Warrick et al. (1997) streamlines did not exhibit this property. The inflection points of (10) at $|x| > x_c$ drift outside the flow domain, i.e. become non-physical.

Obviously, for any $\theta_{0i} > \theta_{0b}$ water accelerates approaching the slanted constant pressure lines, which 'shed' the vertex zone. Symmetrically, for $\theta_{0i} < \theta_{0b}$ the incident flow decelerates near the walls

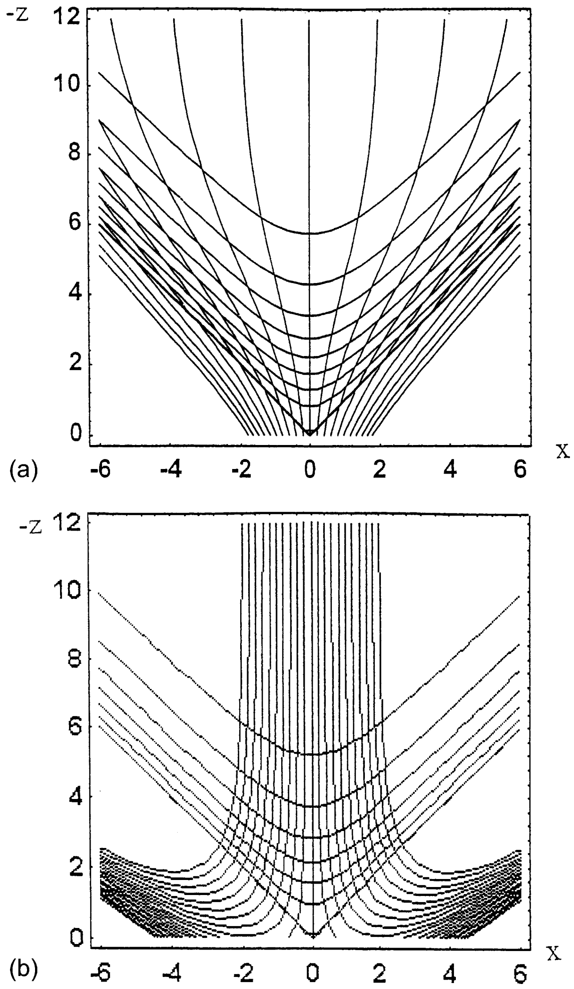

Fig. 2. Flow nets for a symmetrical rectangular trough with (a) $\theta_{0i} < \theta_{0b}$ and (b) $\theta_{0i} > \theta_{0b}$.

and the streamlines 'concentrate' towards B. The same effect was quantified by Philip (1998) for parabolic protrusions.

Warrick et al. (1997) defined the deflection strength of tilted constant pressure surfaces as

$$Q_h = \int_{V_1}^{V_2} u(z)\mathrm{d}z$$

where integration is performed along a vertical line, V_1 is a point on the cap of the left flank in Fig. 1b and V_2 is at infinity. In our case, integration according to Eq. (9) gives

$$q_h(x) = Q_h/(\theta_{0b} - \theta_{0i}) = 1 - \exp(\alpha x), \quad x < 0 \tag{11}$$

According to Eq. (11) the integral deflection decreases towards the corner vertex.

4. 1D limits

Far from point B flow is 1D as it was analyzed by Warrick et al. (1997), i.e. P varies only normally to the tilted wall. Let us obtain this limit from our 2D solution at arbitrary $\gamma_{l,r} < \pi/2$.

Assume in Eq. (7) that $\eta \to \infty$, i.e. move upward-left from the vertex.

Then along the right boundary ($\xi = 0$)

$$u = -\alpha(\theta_{0i} - \theta_{0b})\sin\gamma_l \cos\gamma_l, \quad v = \alpha\theta_{0b} + \alpha(\theta_{0i} - \theta_{0b})\sin^2\gamma_l \tag{12}$$

Obviously, Eq. (12) gives the Ross (1990) formula. From Eq. (12) we conclude that $|u|$ attains its maximum at $\gamma_l = \pi/4$.

One has to be cautious with 1D limits. Indeed, if we proceed to the limit $\gamma_l \to \pi/2$ and $\gamma_r \to \pi/2$ ($\phi_0 \to \pi$), then one might expect to get the 1D infiltration from infinity into a horizontal draining layer (Fig. 1e), which PDE and its solution are

$$\frac{\partial^2\theta}{\partial z^2} - \alpha\frac{\partial\theta}{\partial z} = 0$$

$$\theta_0 = \theta_{0b} + (\theta_{0i} - \theta_{0b})[1 - \exp(\alpha z)], \quad u = 0, \quad v = \alpha\theta_{0b} \tag{13}$$

However, Eq. (4) does not degenerate into Eq. (13). Similarly, in the limit of $\gamma_l \to \pi$, $\gamma_r \to \pi$ and $\phi_0 \to 2\pi$ we would anticipate obtaining the Boussinesq–Sretensky limit of a semi-infinite constant pressure slot (Fig. 1f) when the isobaric lines are confocal parabolas (Sretensky, 1935). This limit has been inspected by Philip and Knight (1989) to be 1D in a parabolic system of coordinates. Again, Eq. (4) does not deliver this limit. Moreover, in the two limits Eq. (4) changes its type from an elliptic PDE to a parabolic one, i.e. the asymptotics with boundary perturbations $\phi \to \pi, 2\pi$ turn out singular. Therefore, our non-orthogonal coordinates (ξ, η) become unsuitable.

5. Refraction

So far we set the constant pressure condition along ABC without any concerns of the fate of the water that infiltrated to the corner boundary. As has been shown by Warrick et al. (1997) and Philip (1998), we can consider the domain under the constant pressure surface as the second porous medium of different physical properties. Then we have to match two flows—in soil II above ABC and in soil I beneath (Fig. 1a). Both soils have the Gardner conductivity and extend sufficiently far from the interface to assure 1D flow conditions at $z \to \pm\infty$. For a parabolic interface, Philip (1998) proved that in soil I flow is collimated i.e. becomes 1D everywhere while the incident flow in soil II is 2D (in Cartesian coordinates) with a vertical alignment of streamlines sufficiently far from ABC. Similar arguments in matching two flows were used in coupling of the two flows by Warrick et al. (1997).

The property of collimation of streamlines seems to be generic for an arbitrary interface between soil I and soil II (Fig. 1a). Indeed, consider a contour AC in Fig. 3a with a constant potential θ_i. Assume that AC can be bounded geometrically by two horizontal lines U–U and L–L. For both flat boundaries kept at the same suction, only a trivial solution to Eq. (1) in the lower half-plane exists i.e. $\theta(x, y) = \theta_i$. Consequently, we surmise that AC in Fig. 3a sandwiched between two horizontal lines generating a trivial solution is doomed to result in the same trivial solution.

Let us consider a tilted interface between two soils (Fig. 3b). Due to collimation in the lower medium, $\theta_{1b} = \theta_{1i}$. To ensure matching of the velocity field (12) in soil II (quasi-linear model parameters k_{s2}, α_2) and the rectilinear flow in soil I (parameters k_{s1}, α_1), we consider a stream line $T_{2i}T_bT_{1i}$. At point T_b pressure p is continuous in the two media but the moisture content jump. Besides, the normal (to the interface) flux at T_b must be continuous (the tangential velocity jumps). As a geometrical consequence, we

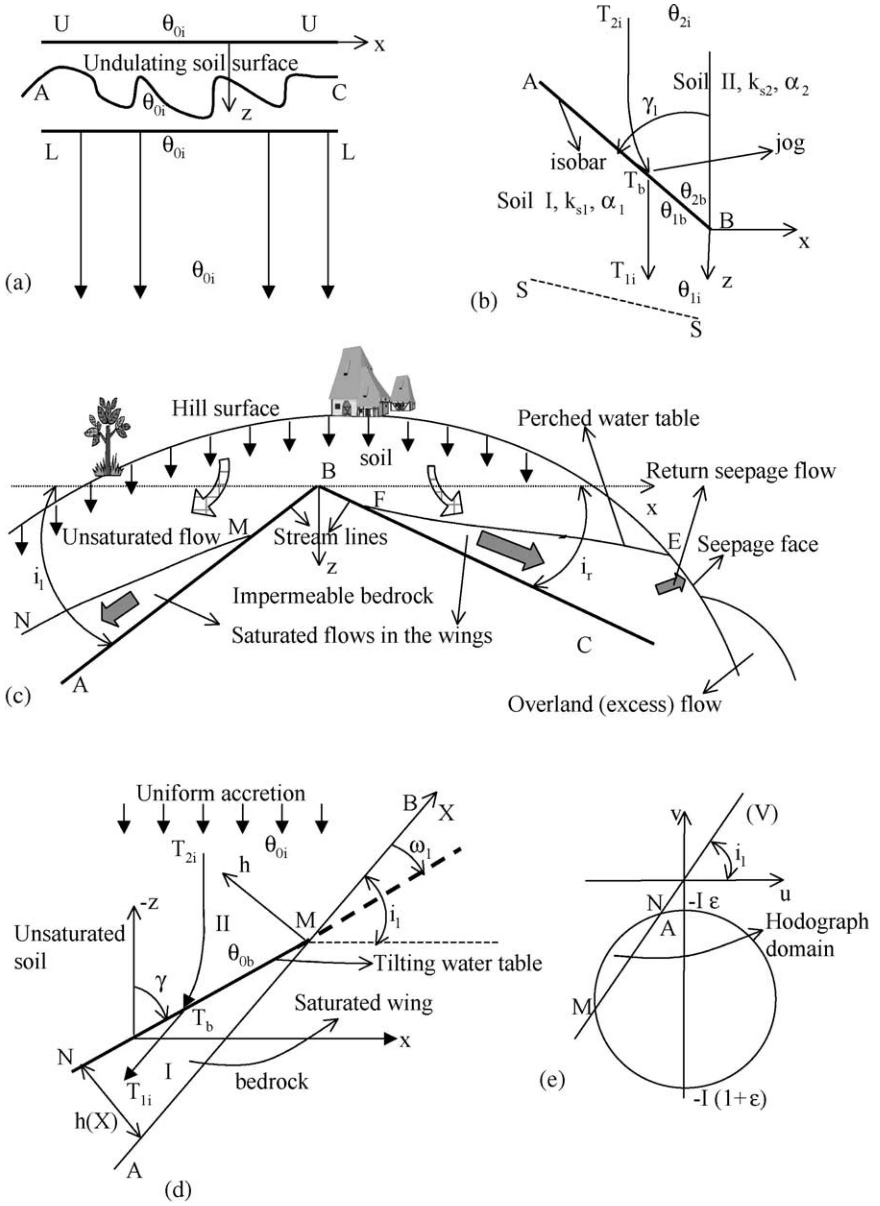

Fig. 3. (a) Arbitrary isobaric contour sandwiched between two horizontal isobars, (b) refraction on a slanted interface, (c) saturated–unsaturated flow in a hillslope, (d) tapering saturated wing, (e) hodograph domain, (f) saturated wing exuding through a seepage face.

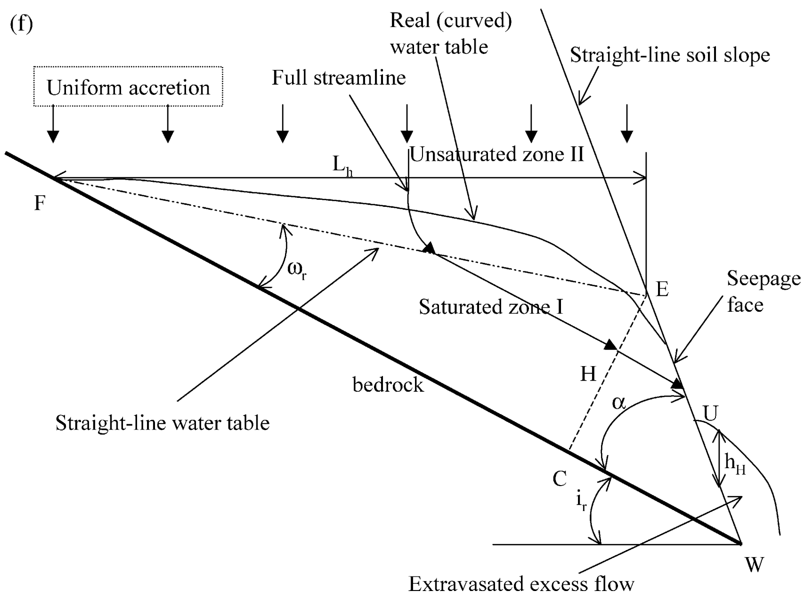

Fig. 3 (*continued*)

have a discontinuity of the stream line slope at T_b. In the Philip model the first jump condition is

$$\left(\frac{\alpha_2\theta_2}{k_{s2}}\right)^{1/\alpha_2} = \left(\frac{\alpha_1\theta_1}{k_{s1}}\right)^{1/\alpha_1} \quad (14)$$

Matching the normal velocities from Eq. (12) and from the trivial solution $u_1 = 0$ and $v_1 = \alpha_1\theta_{1i}$, we come to the second equation

$$\alpha_2\theta_{2i} = \alpha_1\theta_{1i} \quad (15)$$

From Eqs. (14) and (15) at given hydrological conditions (θ_{2i}) and given soil properties, we can easily determine θ_{1i} and θ_{2b}. The latter we set as θ_{0b} in our corner solution above. Clearly, we can consider other slanted or flat interfaces in soil I (Fig. 1b, dashed line $S-S$), in particular, a horizontal water table, i.e. we can combine 'elements' as in Miyazaki (1993) and Warrick et al. (1997). Then, obviously, in the lowest (semi-infinite from below) layer, flow is collimated and in all overlying layers streamlines are curved. Practically, descending moisture reaches the water table (Warrick et al., 1997) located at a depth H in Fig. 1a. Just above a horizontal water table we should match our collimated flow with Eq. (13). If the water table slopes we can again use our solutions as in Section 6.

6. Water table accretion

Saturated and unsaturated flows are matched in two different ways. In groundwater hydrology, infiltration (evaporation) is simulated by a distributed source (sink) over the water table (Polubarinova-Kochina, 1962), i.e. the vadose zone is substituted by a boundary condition along a free surface over a Laplacian domain or a DF saturated sheet (Strack, 1989, pp. 74–89, 243–244, 319–340, 517). In this simplified description, a strictly vertical streamline coming from the unsaturated zone and crossing a non-flat phreatic surface experiences refraction because in the saturated zone the same streamline forms a non-right angle with the phreatic surface (e.g. Todd, 1980, pp. 90–91, Strack, p. 323). Therefore, a streamline in this approximate model intersects the upper boundary of a groundwater mound with a jog similar to one at point T_b in our Fig. 3b. However, in a rigorous saturated–unsaturated flow model (e.g. Tritcher et al., 2001) the hydraulic conductivity is a continuous, albeit not always (in particular, in the Gardner soil) smooth, function of pressure. Hence, streamlines intersecting the phreatic surface should be smooth as is shown in Fig. 3d, line $T_{2i}T_bT_{1i}$. Clearly, in case of a conductivity contrast as in Fig. 3b, streamlines are refracted on the interface that is reflected in both simplified models and the rigorous description.

On the other hand, vadose zone hydrologists often consider the water table as a geometrically flat regional sink for descending flows (Philip, 1989b). Consequently, an atmospheric pressure boundary condition is imposed along the lowest boundary of the unsaturated zone (and the fate of water leaving for the conterminous groundwater zone is neglected).

Philip (1992) and Warrick (1993) investigated in conjunction a 2D Laplacian (saturated) and quasi-linear (unsaturated) flow near a line source (subsurface emitter) with a free surface (oval-shaped 'water table') appearing as a part of the solution. Here we use the same Philip–Warrick idea of 2D conjugation but we focus on the generic scheme in hillslope hydrology when a perched water table is formed on a 'sloping slab' (e.g. Dingman, 1994, pp. 415, 419, 422).

The hydrology of hillslopes is complicated due to 3D effects, heterogeneity of the matrix, transience of recharge events, topographical irregularities, etc. (Kirkby, 1985; Zaslavsky and Sinai, 1981) that brings about a flow topology with intermittent recharge–discharge zones, hinge lines, stagnation points, etc. (Sophocleous, 2002). However, even for simple schemes matching of saturated and unsaturated hillslope flows has been done numerically (Dingman, 1994, Tritcher et al., 2001). We shall give a lucid example of analytical closed-form matching of our solution (12) with a DF flow.

We consider an impervious dome *ABC* (bedrock) protruding into the soil. Soil surface is exposed to infiltration of a given intensity. We assume that the thickness of the soil cover is high enough for formation of uniform infiltration, which bifurcates near the dome crest.

It is well-known (Philip et al., 1989) that the stream function ψ in the quasi-linear model satisfies the same Eq. (2) as the Kirchhoff potential. That makes possible considering impermeable boundaries like *BM* and *BF* in Fig. 3c along which $\psi = \text{const}$. Boger (1998), Philip (1988), Philip and Knight (1989), Philip et al. (1989), Warrick and Fennemore (1995) and Zachman (1978) investigated analytically finite and semi-infinite impermeable boundaries (inclined bottoms, protrusions, cavities, Rankine-type stones, etc.). In domains unlimited from above, an obvious asymptotic $\psi \sim \alpha\theta_{0i}x$ at $z \to -\infty$ holds. An elegant analytical solution for a single 'critical' (i.e. both constant potential and no-flow) protuberance has been recently found by Youngs (2002) in terms of a capillary-fringe model based on the theory of holomorphic functions.

However, if we place an impervious corner like *ABC* in Fig. 1c into a uniform descending flow, there will be no solution for purely unsaturated conditions. Needless to say that if we position a trough directing its impervious arms upward, then quasi-linear flow is also impossible. This fact becomes vital if instead of truly impervious boundaries (e.g. stones or domes) one models so-called subcritical structures (tunnels) for which the non-existence of unsaturated flows practically implies trickling through some parts of the tunnel contour (Kacimov, 2000). We conjecture that the Philip and Knight (1989) parabola is the bluntest semi-infinite body that supports a purely unsaturated quasi-linear infiltration flow.

Two saturated 'wings' form on the two sides of the corner in Fig. 3c. Here *NM* and *EF* are perched water tables. The right wing (with through flow in terms of Kirkby, 1985) exudes through the hill slope. What seeps out is called the return flow (Sophocleous, 2002), which, if intensive enough, can generate the overland excess flow. If the infiltration rate is high enough (or the two soil flanks above the dome dip at sufficiently small angles i_l and i_r), then the two 'wings' merge and the crest *B* is capped by a single-branched phreatic surface. This regime will not be studied here. We shall consider only the disjoint wings as in Fig. 3c.

In Dingman (1994), all perched water tables on slanted bedrocks are shown as straight (tilted) lines. Our analysis will corroborate this configuration. We seek, first, a solution for the left water table *NM* in Fig. 3d, that is a ray originating at *M* to which the saturated zone tapers. We set a longitudinal coordinate X along *MB* and transverse coordinate h normal to X. In the saturated zone I, we assume the DF model (Chapman and Dressler, 1984; Verhoest and Troch, 2000), i.e. we suppose that in *AMN* the groundwater velocity and hydraulic head depend on X only (lines perpendicular to the bed are constant head lines). Along *NM*, a uniform recharge $E = \alpha\theta_{0i}$ from the quasi-linear zone II takes place.

Let us start with zone I. The thickness $h(X)$ of the saturated wing satisfies the ODE

$$\cos i_l \frac{\mathrm{d}}{\mathrm{d}X}\left(h\frac{\mathrm{d}h}{\mathrm{d}X}\right) + \sin i_l \frac{\mathrm{d}h}{\mathrm{d}X} + \epsilon = 0 \tag{16}$$

where $\epsilon = E/k_s$. Instead of Eq. (16) adopted from Verhoest and Troch (2000), we can use a more adequate equation from Chapman and Dressler (1984, Eq. (80)), which, however, is mathematically equivalent to Eq. (16) because the two equations differ in constant coefficients only.

We search for a solution to Eq. (16) in the form $h = aX + b$ where a and b are two constants, i.e. for a straight-line water table. The water table inclination angle (counted positively clockwise from the X axis) is $a = -\tan\omega_l$. We can set $b = 0$ due to the coincidence of the origin of coordinates and the perched zone tip. Putting aX into Eq. (16) we arrive at the following quadratic equation for a

$$\cos i_l a^2 - \sin i_l a + \epsilon = 0 \tag{17}$$

We select the root

$$a_1 = -\tan\omega_l = \frac{-\sin i_l + \sqrt{\sin^2 i_l - 4\epsilon\cos i_l}}{2\cos i_l} \tag{18}$$

From Eq. (18) the condition for solving Eq. (17) is $\sin^2 i_l > 4\epsilon\cos i_l$, i.e. as we have emphasized, to generate a stable perched groundwater wedge either the bedrock slope should be steep or infiltration small. If this inequality is not satisfied, no steady regime is possible. More precisely, the wing will grow transiently and eventually flow out through a discharge zone as in the right half of Fig. 3c. If the soil surface is flat and we do not provide a vent for the saturated wedge to escape, it will expand into the whole soil volume and (under continued precipitation) surface flooding will take place. Obviously, if $i = 0$ in Eq. (17), viz. the bedrock is horizontal, then a straight-line steady solution does not exist, and one has to search for a solution $h^2 = a_1X^2 + a_2X + b$ which leads to an elliptical water table (Polubarinova-Kochina, 1962).

Even if the most rigorous hydrodynamic model (Polubarinova-Kochina, 1962) is applied to the saturated 'wing' assuming a 2D flow in zone I, the problem can have no steady-state solutions. In this model the water table is not necessarily straight, and the Polubarinova-Kochina methods of hodograph and linear differential equations can be used to find its shape. According to these two methods, we deal with the hodograph plane $V = u + \mathrm{I}v$ where $V(u, v)$ is the saturated specific discharge (related to k_s) and I is the imaginary unit. In this plane, the image of a phreatic surface with accretion is a circle of a unit radius centered at the point $-\mathrm{I}(\epsilon + 1/2)$ (see Polubarinova-Kochina, 1962 for details) and the image of the bedrock AM is a straight line as it is shown in Fig. 3e. The hodograph domain corresponding to the physical flow domain is a segment MNA (points N and A merge) and is identical to the domains in oil–gas trap hydrodynamic models (Kacimov and Obnosov, 2001). If we decrease i_l (spinning MA clockwise about the origin of coordinates) or increase ϵ (shifting the hodograph circle downward), then we reach the limiting case when MA merely touches the circle and the hodograph degenerates into one point that implies a uniform flow with a straight tilted free surface. At even higher ϵ (or lower i_l) the wing does not exist (analogously to Kacimov and Obnosov, 2001). The critical value from the hodograph in Fig. 3e is $\tan i_c = 2\sqrt{\epsilon}/(1-\epsilon)$. Comparing this limit with one delivered by the hydraulic model (18) we conclude that the DF and hydrodynamic models give fairly close solvability criteria.

Now we consider flow in zone II. In the vicinity of point M, we have a constant potential condition along MN and no-flow condition along MB. Unfortunately, we cannot yet solve a mixed boundary-value problem of this type for Eq. (1). However, far from point M in Fig. 3d we can apply our solution (12) for a tilted isobar MN. We only have to put $\theta_b = \theta_s$ in Eq. (12) because MN is the water table. Then from Eq. (12) $v/u = \tan i_l$, i.e. upon entering the saturated zone, flow lines get collinear with the bedrock. Hence, we arrive at a quadratic equation for $\tan\gamma$, the roots of which are

$$\tan\gamma = \frac{(1-\epsilon)\tan i_l \pm \sqrt{(1-\epsilon)^2\tan^2 i_l - 4\epsilon}}{2\epsilon} \tag{19}$$

We select " $-$ " in Eq. (19). In Eq. (18) $\omega_l = \gamma + i_l - \pi/2$, and we can compare the DF and quasi-linear models. Curves 1 and 2 in Fig. 4 depict two pairs of curves $\tan\gamma(i)$ at $\epsilon = 0.05$ and $\epsilon = 0.1$ according to Eqs. (18) (upper curves in the pairs) and (19) (lower curves). In Fig. 5 we illustrate the dependence $\tan\gamma(\epsilon)$ at $i = \pi/8$ and $i = \pi/4$. As we can see in

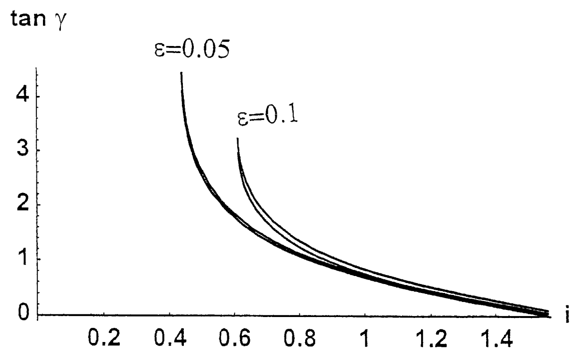

Fig. 4. Water table angle as a function of the bedrock angle for two infiltration rates.

the graphs, at practically reasonable slopes and infiltration rates, the curves are quite close that supports our assumption on effectively uniform source (recharge) in the DF model (16). We underscore that zones I and II in Fig. 3d are inherently coupled: without infiltration, the wedge would disappear and without the wedge quasi-linear steady infiltration is mathematically impossible.

Let us consider the right half of Fig. 3c zoomed for clarity as Fig. 3f. We assume that the soil slope is a straight line plunging at an angle $\alpha + i_r$. Due to infiltration, a curved water table is formed. Groundwater seeps out through a seepage face *EU* and a segment *UW* of the slope, which is covered by the Hortonian sheet flow. The thickness of this flow (if any) h_H is small and we assume that along *EW* pressure is atmospheric. Next, we approximate the real water table by a straight line one (*EF*) and set a straight line *EC* normally to the bedrock. The locations of point *E* on the slope and point *F* on the bedrock are now unknown.

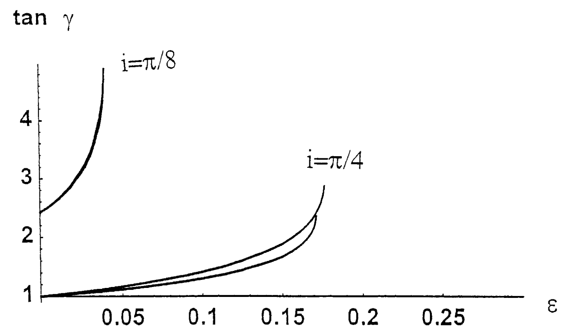

Fig. 5. Water table angle as a function of infiltration rate at two bedrock dips.

The saturated zone triangle I in Fig. 3f can be decoupled into two parts: a rectangular triangle capped by a phreatic surface *EFC* and a rectangular triangle *ECW*. Then in *EFC* we can again adopt the DF model (16) and our solution. Obviously, *EC* is a constant head boundary. Therefore, in *ECW* we have exactly the same flow conditions as in Youngs (1974), Fig. 3. In this *ECW* triangle, groundwater flow is rigorously parallel to the bedrock that follows from the full hydrodynamic (2D) model (Polubarinova-Kochina, 1962). Thus, flow in the two triangles is perfectly matched. According to Youngs (1974), the exuding rate through *EW* is

$$Q = k_s H(\sin i_r + \cos i_r \tan \alpha)$$

where $H = |EC|$. Due to our uniform accretion assumption, the recharge rate through *EF* is

$$Q = \epsilon k_s L_h = \epsilon k_s H(\sin i_r + \cos i_r \tan \omega_r)$$

From the last two expressions H, Q and *EF* can be found easily.

In Fig. 3c we can see the importance of the bedrock obliquity and corresponding ω. In studying groundwater ridging (Sophocleous, 2002), one should collect the data on i (along with standard porosity–conductivity measurements of the slope soil). As shown in Fig. 3c, the right saturated wing discharges through the slope (gently dipping rock) while the left wing has no outwardly detectable signs of seepage, although both wings are characterized by the same soil, precipitation and topography.

7. Discussion and unresolved problems

We obtained new analytical solutions for unsaturated and saturated corner-type zones. Infiltration flow is proved to be deflected by subsurface troughs, which mimic irregular interfaces common in sedimentation of rocks, genesis of soils, or purposely crenellated buried geotechnical gravel packs or liners.

By matching two corner flows in a hillslope, we fine-tuned the common model of Todd (1980) for infiltration recharging a tilted water table. We demonstrated that the vertical streamlines from the vadose zone are not refracted by the free surface. Trajectories of water particles passing through the phreatic surface, are smooth. Figuratively speaking, the groundwater stream entrains the infiltration flow even above the phreatic surface, i.e. the saturated zone has an effect that extends upward (although deflection of unsaturated stream lines occurs just above the water table). Chapman and Dressler (1984) reasoned that this deflection is by means of 'effective' turning of the infiltration vector near the water table; however, they did not do rigorous matching of the saturated and vadose zone. In summary, vertical recharge arrows common in most hydrological textbooks should be drawn with 'turned heads'.

We used the Philip quasi-linear model and the advective-dispersion Eq. (1) for the Kirchhoff potential. We explored only the simplest 2D solution to this equation in a corner. For a right angle trough at an arbitrary orientation we contrived to separate the variables in an elliptic PDE that allowed us to circumvent even a standard Fourier integration over the separation constant variable. The Fourier method (Polubarinova-Kochina, 1962) can be implemented if, for instance, our corner problem in Fig. 1c is generalized to the case of a 'bent' of a thickness d (Fig. 6a). In the arm-aligned coordinates this bent is a square $0 \leq \xi \leq d$, $0 \leq \eta \leq d$. It would be also interesting to consider three-medium systems with a bent semi-permeable seam of a small thickness d (Fig. 6a) modeling a thin geomembrane located between two unsaturated lumps.

If ϕ_0 in Fig. 1c is not a right angle, then the mixed second derivative in Eq. (4) persists, and the two variables do not separate as $F_m G_m$. Nonetheless, we can search for normal mode solutions

$$\theta_m = \exp(-a_m \xi)\exp(-b_m \eta) \qquad (20)$$

For the mode coefficients a_m and b_m we get a quadric form (Pinsky, 1991) and a spectrum of roots $m = 1, 2, \ldots$ satisfying the corresponding equation. At $\phi_0 < \pi$ we can attempt to fit both boundary and infinity conditions for θ by combining linearly θ_m.

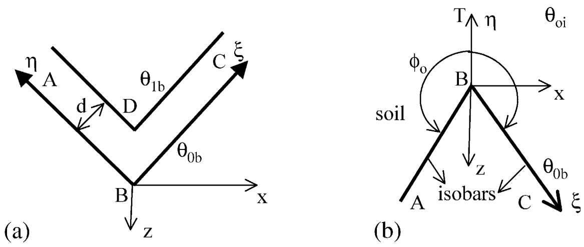

Fig. 6. (a) Bent seam, (b) sharp-crested protrusion.

For $\phi_0 > \pi$ the form (20) is not suitable because we have zones where ξ or η are negative, i.e. the infinity condition cannot be satisfied by normal modes. Still, for symmetric corners with $\gamma_l = \gamma_r$ we can select other non-orthogonal coordinates shown in Fig. 6b such that one axis coincides with the corner side and another-with the axis of symmetry BT. Then in TBC the condition $(\xi, \eta) \geq 0$ holds and we can try Eq. (14) as normal modes. The only difference with $\phi_0 < \pi$ will be in the boundary condition along BT, where $u = 0$ instead of $\theta = 0$.

Analytical solutions for arbitrary constant pressure corners would allow us to assemble them as elements (Strack, 1989) and to model the whole interface in Fig. 1a. Of special importance would be an analytical solution for an arbitrary (non-constant pressure) Dirichlet problem (even in a solitary corner). A mixed boundary-value problem for Eq. (1) seems to be prohibitively complicated because even in a half-plane (e.g. Fig. 1e), mathematicians have not yet supplied for Eq. (1) anything resembling the Signorini formula available in saturated conditions (Polubarinova-Kochina, 1962).

Acknowledgements

This study was conducted as a part of the project IG/AGR/SOIL/02/04, Sultan Qaboos University. Helpful comments and criticism of I. Leyen, M. Sophocleous, A. Warrick and an anonymous reviewer are appreciated.

References

Boger, M., 1998. Solutions of unsaturated seepage problem by power-series method. J. Hydrol. Engng, ASCE 3, 182–192.

Cedergren, H.R., 1989. Seepage, Drainage and Flow Nets, Wiley, New York.

Chapman, T.G., Dressler, R.F., 1984. Unsteady, shallow groundwater flow over a curved impermeable boundary. Water Resour. Res. 20, 1427–1434.

Concer, D.B., 1959. Heat flow towards a moving cavity. Q. J. Mech. Appl. Math. 12, 222–232.

Dingman, S.L., 1994. Physical Hydrology, Prentice Hall, Upper Saddle River.

Gardner, W.R., 1958. Some steady-state solutions of the unsaturated moisture flow equation with application to evaporation from a water table. Soil Sci. 85, 228–232.

Kacimov, A.R., 2000. Circular isobaric cavity in a descending unsaturated flow. J. Irrig. Drain., ASCE 126, 172–178.

Kacimov, A.R., Obnosov, Yu.V., 2001. Analytical solutions to hydrodynamic problems for oil and gas traps. J. Hydrol. 254, 33–46.

Khire, M.V., Benson, C.H., Bosscher, P.J., 2000. Capillary barriers: design variables and water balance. J. Geotech. Geoenviron. Engng, ASCE 126, 695–708.

Kirkby, M.J., 1985. Hillslope hydrology. In: Anderson, M.G., Burst, T.P. (Eds.), Hydrological Forecasting, Wiley, Chichester, pp. 37–75.

Miyazaki, T., 1993. Water Flow in Soils, Dekker, New York.

Morse, P.M., Feshbach, H., 1953. Methods of Theoretical Physics, Pergamon, New York.

Philip, J.R., 1969. Theory of infiltration. Adv. Hydrosci. 5, 215–296.

Philip, J.R., 1984. Steady infiltration from circular cylindrical cavities. Soil Sci. Soc. Am. J. 48, 270–278.

Philip, J.R., 1988. Steady unsaturated seepage above a sloping impermeable base. Water Resour. Res. 24, 1192–1196.

Philip, J.R., 1989a. The scattering analog for infiltration in porous media. Rev. Geophys. 27, 431–448.

Philip, J.R., 1989b. Multidimensional steady infiltration to a water-table. Water Resour. Res. 25, 109–116.

Philip, J.R., 1990a. Some general results on the seepage exclusion problem. Water Resour. Res. 26, 369–377.

Philip, J.R., 1990b. Conjectures on certain boundary-layer equations and natural coordinates. Proc. R. Soc. Lond. A 428, 307–324.

Philip, J.R., 1991. Hillslope infiltration: planar slopes. Water Resour. Res. 27, 109–117.

Philip, J.R., 1992. What happens near a quasi-linear point source? Water Resour. Res. 28, 47–52.

Philip, J.R., 1998. Seepage shedding by parabolic capillary barriers and cavities. Water Resour. Res. 34, 2827–2835.

Philip, J.R., Knight, J.H., 1989. The seepage exclusion problem for parabolic and paraboloidal cavities. Water Resour. Res. 25, 605–618.

Philip, J.R., Knight, J.H., Waechter, R.T., 1989. Unsaturated seepage and subterranean holes: conspectus, and exclusion problem for circular cylindrical cavities. Water Resour. Res. 25, 16–28.

Pinsky, M.A., 1991. Partial Differential Equations and Boundary-value Problems with Applications, McGraw-Hill, New York.

Polubarinova-Kochina, P.Ya., 1962. Theory of Ground Water Movement, Princeton University Press, Princeton.

Protter, M.H., Weinberg, H.F., 1984. Maximum Principles in Differential Equations, Springer, New York.

Ross, B., 1990. The diversion capacity of capillary barriers. Water Resour. Res. 26, 2625–2629.

Sherman, F.S., 1990. Viscous Flow, McGraw-Hill, New York.

Sisavath, S., Jing, X., Zimmerman, R.W., 2001. Laminar flow through irregularly-shaped pores in sedimentary rocks. Transport Porous Media 45, 41–62.

Sophocleous, M., 2002. Interactions between groundwater and surface water: the state of the science. J. Hydrogeol. 10, 52–57.

Sretensky, L.N., 1935. Sur le rechauffement des fluides par des corps solides. Prikl. Math. Mekh. 2, 163–179.(in Russian, with abstract in French).

Strack, O.D.L., 1989. Groundwater Mechanics, Prentice Hall, Englewood Cliffs.

Todd, D.K., 1980. Groundwater Hydrology, Wiley, New York.

Tritcher, P., Read, W.W., Broadbridge, P., Knight, J.H., 2001. Steady saturated–unsaturated flow in irregular porous domains. Math. Comput. Model. 34, 177–194.

Verhoest, E.C., Troch, P.A., 2000. Some analytical solutions of the linearized Boussinesq equation with recharge for a sloping aquifer. Water Resour. Res. 36, 793–800.

Waechter, R.T., Philip, J.R., 1985. Steady two- and three-dimensional flows in unsaturated soil: the scattering analog. Water Resour. Res. 21, 1875–1887.

Warrick, A.W., 1993. Unsaturated–saturated flow near a quasi-linear line source. Water Resour. Res. 29, 3759–3762.

Warrick, A.W., Fennemore, G.G., 1995. Unsaturated water flow around obstructions simulated by two-dimensional Rankine bodies. Adv. Water Resour. 18, 375–382.

Warrick, A.W., Wierenga, P.J., Pan, L., 1997. Downward water flow through sloping layers in the vadoze zone: analytical solutions for diversions. J. Hydrol. 192, 321–337.

Youngs, E.G., 1974. Seepage rates and the horizontal flow approximation. Water Resour. Res. 10, 874–876.

Youngs, E.G., 2002. The seepage exclusion problem for tunnel cavities in the saturated capillary fringe. In Environmental Mechanics: Water, Mass and Energy Transfer in the Biosphere. Geophysical Monograph, 129, pp. 71–78. American Geophysical Union

Zachman, D.W., 1978. A mathematical treatment of infiltration from a line source into an inclined porous medium. Soil Sci. Soc. Am. J. 42, 685–688.

Zaslavsky, D., Sinai, G., 1981. Surface hydrology: IV. Flow in sloping, layered soil. J. Hydraul. Engng., ASCE 107, 53–64.

Zauderer, E., 1989. Partial Differential Equations of Applied Mathematics, Wiley, Singapore.